Int. J. Solids Structures, 1976, Vol. 12, pp. 159–171. Pergamon Press. Printed in Great Britain

FUNDAMENTAL EXPERIMENTS IN PLASTICITY AND CREEP OF ALUMINUM—EXTENSION OF PREVIOUS RESULTS†

A. PHILLIPS and M. RICCIUTI
Department of Engineering and Applied Science, Yale University, New Haven, CT 06520, U.S.A.

(*Received* 3 *March* 1975; *revised* 4 *August* 1975)

Abstract—Paper presents combined stress experiments in plasticity and creep of aluminum 1100-0. The purpose of these experiments was to determine the motion of the yield surface in tension-torsion space for three complicated prestressing paths, to investigate the validity of the normality hypothesis, to investigate the development of creep strains after prestressing, and finally to investigate the validity of the constant volume hypothesis.

It is shown that the law of hardening proposed by the author previously [3, 5, 6] is valid, except possibly when the prestress path intersects the yield surface at a small angle. It is also shown that the normality hypothesis is valid. After prestressing the creep strain vector has in the beginning the same direction as the plastic strain vector but later its direction may change. Finally it is shown that at the level of permanent strains less than 1% the plastic strains follow the constant volume hypothesis but the creep strains do so only when they begin to appear.

INTRODUCTION

In this paper we continue the presentation of experimental results concerning the foundations of plasticity at room and at elevated temperatures. We present an extension of previous work by the senior author and his associates [1–5] on commercially pure aluminum 1100-0. The purpose of the present experiments were (1) to determine the motion of the yield surfaces in the tension-torsion space for three complicated prestressing paths, (2) to determine the direction of the plastic strain vector along the prestressing path and the validity of the normality assumption between the yield surface and the plastic strain rate vector, (3) to investigate the development of creep after prestressing, and (4) to investigate whether at the level of permanent strains less than 1% the plastic strains and the creep strains satisfy the constant volume hypothesis.

The yield surfaces obtained in this paper were based on the proportional limit definition of yielding. The practical procedure in obtaining the proportional limit and the yield surfaces has been described in [2, 3]. We found that our procedure gives values unaffected by the slight penetration of the plastic region as long as this penetration is no more than ≈ 3 μmin/in. This procedure is conceptually different from the offset method since in our case the proportional limit is the value of the stress obtained by linearly extrapolating from the stress corresponding to the agreed upon offset value to a stress corresponding to a zero offset. This definition of yielding is the basis for the hardening law presented in [3], expanded in [5], and analytically expressed in [6]. We restate this law since it will be used in the evaluation of our experiments. It should be added that if a (non-zero) offset definition of yielding were used the above law would not have been experimentally verified because of the inevitable distortion in the yield surface due to the influence of the amount of offset. This distortion is also predictable from the discussion in [19].

The hardening law is as follows, Fig. 1. Suppose C_i is the yield curve at the level of prestressing P_i. If starting from within the elastic region bounded by C_i a new prestressing path ending at P_{i+1} produces a new yield curve C_{i+1}, then C_{i+1} can be derived from C_i by a superposition of two motions in the direction of prestressing, a rigid body translation $C_i \rightarrow C'_{i+1}$ and a deformation $C'_{i+1} \rightarrow C_{i+1}$.

One of the purposes of the present experiments is to test the validity of the the above hardening law for prestressing paths more complicated than the ones presented in previous papers. We believe that this hardening law represents within limits the real behavior of aluminum 1100-0 and possibly of other metals, and therefore should be derivable from microstructural considerations. The region of its applicability is a large class of prestressing paths and the limits of its applicability should be determined rationally. In the absence of a derivation of this

†This research was supported by an NSF Grant to Yale University.

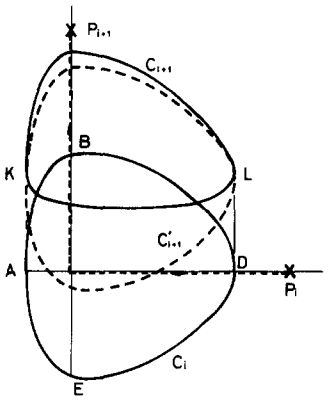

Fig. 1. The hardening rule.

hardening law from microstructural considerations it is necessary to experiment with many complicated prestressing paths. Our experiments have shown that the proposed hardening law is valid for the prestressing paths used in these experiments, except possibly when the prestress path intersects the tangent plane to the yield surface at a small angle.

The hardening law investigated here is a generalization of the concept of the lack of cross effect presented by Naghdi *et al.*[7] for prestressing in torsion. This law is quite different from hardening laws introduced previously by other authors, as for example, by Prager[8], Ishlinskii[9], Hodge[10], Ziegler[11] and Baltov and Sawczuk[12]. The experimental determination of yield surfaces for several metals has been the subject of a number of previous investigations by other authors, such as Naghdi *et al.*[7], Ivey[13], Batdorf and Budiansky[14], Taylor and Quinney[15], Miastkowski and Szczepinski[16], Mair and Pugh[17], to name a few. All these investigations were performed at room temperature. The present investigation, as well as all others performed by the senior author and his colleagues were devoted to both room and elevated temperatures and the hardening law considered by us is shown to be valid also at elevated temperature. The only other investigation at elevated temperature known to the authors is that of Brown[20].

In addition to the determination of the boundary of the elastic region at different prestressing levels and for different prestressing paths, the present investigation determined the direction of the plastic strain path in the plastic strain space and compared it to the stress path in the stress space. Thus, the direction of the plastic strain rate vector could be obtained at different stages during the prestressing process. It was possible to infer that normality between yield surface and plastic strain rate vector is valid when the prestress path crosses the yield surface in order to produce a new prestress or at the endpoint of a prestress path. In addition if we assume that normality is valid throughout prestressing then by determining the direction of the plastic strain vector we simultaneously determine the manner in which the element of the yield surface in the neighborhood of the plastic strain rate vector is moving as prestressing progresses.

At the end of a prestressing period it is possible to either re-enter the new elastic region immediately, thus effectively terminating all plastic deformation, or remain at the prestressing point while creep deformation develops and finally stops. Both procedures were followed here. We succeeded to determine the effect of each procedure on the yield surface. We also succeeded to show how the creep which developed while the state of stress was stationary at the prestressing point, did affect the direction of the creep strain vector.

A number of tests were made in which we investigated the validity of the constant volume hypothesis for plastic strains and creep strains when the deformation level is less than 1%. We found that while plastic strains followed the above hypothesis, creep strains do so only in the beginning of the creep period.

EXPERIMENTAL TECHNIQUE

The experiments, on commercially pure aluminum 1100-0, were made with tubular specimens described in[2] and loaded in combined tension and torsion, and with specimens of square cross section, Fig. 2, loaded in tension only. The tubular specimens were machined from tubular

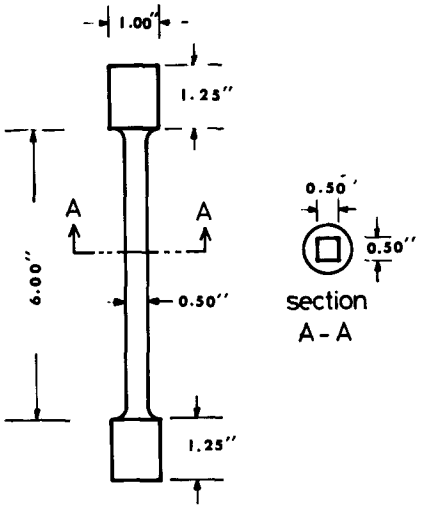

Fig. 2. Typical specimen of square cross section.

extruded rods and annealed at 650°F for 2 hr and then furance-cooled to room temperature. The square cross section specimens were machined from solid extruded rods; specimens RA-1, RA-3, RA-4 were annealed as the tubular specimens, but specimens RA-5, RA-6, RA-7 and RA-8 were annealed at 1000°F for 2 hr and furnace cooled to room temperature.

The testing machine was of the deadweight type allowing the incremental rate of loading to be controlled. It can be used to apply axial, torsion, and reverse torsion loads at variable temperature. A description of the testing machine is given in [2]. Improvements to the testing machine consisted in the use of new high precision universal joints with needle bearings, replacement of the old pulleys with new high precision ones of a much larger diameter, and reduction in the number of pulleys from 14 to 10. In this way the frictional losses were reduced from 8 psi in 2000 psi shear stress, to 1 psi in 2000 psi shear stress.

For the testing program on the square specimens the tension pan was rotationally uncoupled from the specimen by the use of a high precision needle thrust bearing and it was dampened for oscillations through the use of foam rubber dampers lightly resting against the bottom of the tension pan. These dampers did not influence the applied load. The experiments with the square specimens required torque uncoupling since the torsional rigidity of the specimens was very low and tension pan oscillations would conceivably cause unwanted yielding.

Tensile stress change was generated through increments of 50 lb weight added or subtracted from the tension pan (corresponding to 150 psi axial stress for the tubular specimens and to 200 psi axial stress for the square cross section specimens). For the tubular specimens shearing stress change was generated through increments of 2 lb weight added or subtracted from the torsion pan (corresponding to ~100 psi shearing stress).

Four strain gages were bonded, as indicated in [2], to the outer surface of the specimens at middle length in locations 90° from one another. These gages were 45° rosette BLH-FABR-50-12S13 for the tubular specimens. For two symmetrically located gages on the square cross section specimens they were 45° rosette BLH-FABR-25-12S13. The remaining two gages for the square cross section specimens were 90° rosette BLH-FABX-25-12S13 type. The details of the strain gage orientations and the connections into the Wheatstone bridge circuits for the tubular specimens are shown in Fig. 3. These are different from the ones used in [1–3]. The advantages of the gage connections into the Wheatstone bridge circuit used for the tubular specimens over the previously used ones are increased strain sensitivity and decreased temperature sensitivity. For the shearing strain measurements the sensitivity was 1/4 μin/in, and for the axial and hoop strain measurements the sensitivity was $1/2(1+\nu)$ μin/in, where ν is the Poisson's ratio.

For the tubular specimens each Wheatstone bridge was connected to a BLH model 80306 signal conditioner, consisting of a variable gain normalizing amplifier, a power supply for bridge excitation, and a digital voltmeter. To insure long time stability each amplifier was modified using an analog gate circuit to give zero drift.

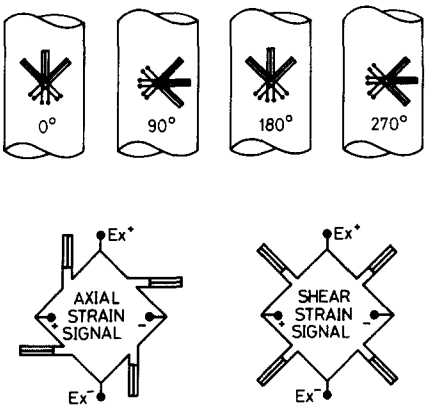

Fig. 3. Tubular Specimens: Strain gage orientations and connections into the Wheatstone bridge circuits.

The axial and transverse gages of the square cross section specimens were connected in the conventional single active arm Wheatstone bridge circuit. Each strain signal was fed into a BLH model 3602 signal conditioner with excitation supplied by a BLH model 3584 power supply. The output from the signal conditioner was fed into a Doric Digitrend model 210 data acquisition system which included the same self-zeroing feature outlined previously. The four shear strain gages of these square cross section specimens were connected in the four arm active bridge circuit. The readability for the square cross section specimen strains was 1/2 μin/in for axial and transverse stains and 1/8 μin/in for the shear strains.

The temperature of the specimen was increased by heat conduction and it was measured by thermocouples of the beaded junction type and a strip chart recorder[1, 2]. In order to increase the temperature measurement accuracy the thermocouples were sampled at frequent intervals. A switch box permitting rapid sampling of the thermocouples was constructed and used.

The tubular specimens were used for obtaining yield surfaces and the plastic and creep strain vectors. The specimens with square cross sections were used for a verification of the constant volume hypothesis for plastic and creep strains. As in[1–3] it was decided to use only one specimen for the determination of the entire virgin yield surface and its subsequent yield surfaces. In order to obtain each indication of yield it is necessary to probe into the plastic region and therefore deform the yield surface while trying to determine it. Consequently, when only one specimen is used it is necessary to restrict each incursion into the plastic region to extremely small values and therefore the proportional limit definition of yielding must be used. In these experiments, due to improvements in the instrumentation compared to our previous tests[1–3] each incursion into the plastic region was limited to approx. 2 μin/in plastic strain (equal to eight times the readability of the instrumentation).

The precise definition of yielding used in these experiments has been described repeatedly in[1–3] and is essentially the proportionality limit definition.

After a positive or negative loading increment was applied, 3 min were allowed to lapse until the next loading increment would be applied. All strain readings were allowed to stabilize before recording.

In most of the tests the specimen were prestressed to a particular value of the stress, then unloaded along the prestress path to a stress within the new elastic region; the specimen was not permitted to stay for more than 3 min at the prestressing value. This was the method also used in the previous tests[1–3]. However, in some of our tests, the specimen was allowed to remain at the prestressing point for an extended period of time before retreating within the elastic region or before nearly complete unloading.

Whenever a change of temperature was needed, the rate of temperature change was 3°F/min.

RESULTS-THE MOTION OF THE YIELD SURFACE AND THE QUESTION OF NORMALITY

In this section we shall present the results of tests with three specimens concerning the motion of the yield surface due to prestressing as well as the normality between the plastic strain rate vector and the yield surface.

Specimen R-3. In this experiment we succeeded with the same specimen to obtain an initial and seven subsequent yield surfaces. All prestressings were at 75°F.

Figure 4 shows the yield curves at the indicated temperatures for the initial yield surface as well as for the first three subsequent yield surfaces. The specimen was prestressed to the point A ($\sigma = 6500$ psi, $\tau = 0$ psi, $\epsilon_x^{pl} = 220$ μin/in) then immediately unloaded to within the yield surface. Then the first subsequent yield surface was obtained by means of four yield curves at the indicated temperatures. Several of the yield points at each yield curve were duplicated even after obtaining the appropriate yield curve, and in many cases after obtaining all the yield curves at all temperatures. A perfect agreement was obtained which proves that the method of yield determination does not change the yield surface.

Next the specimen was subjected to a second prestressing by unloading in axial stress to the point B ($\sigma = 1060$ psi, $\epsilon_x^{pl} = 5$ μin/in). After reaching the point B the specimen was immediately reloaded within the new elastic region. The second subsequent yield surface was obtained by means of two yield curves at 75 and 150°F.

Next the specimen was prestressed to the point C ($\sigma = 1800$ psi, $\tau = 3290$ psi, $\gamma_{xy}^{pl} = 60$ μin/in. Then the specimen was immediately unloaded within the new elastic region. Then the third subsequent yield surface was obtained by means of two yield curves.

Up to now the results were similar to those reported in [18], Specimen R-2, where the path of loading was the same. We can observe (1) a complete lack of cross effect, as in [1–5], (2) that the subsequent yield curves decrease (increase) in width in the prestress direction for loadings away from (towards) the stress origin, as in [1–5].

Since prestressing away from the origin tends to decrease the width of the yield curve in the prestress direction, while prestressing towards the origin tends to increase the width of the yield curve in the prestress direction the concept of the global neutral loading was proposed in [5, 18]. For such a loading the width of the yield surface in the direction of the prestressing will not change. The fourth and fifth prestressings of test R-3 were devoted to an initial attempt to find whether the Mises surface represents such a global neutral loading surface. Figure 5 illustrates the experimental results for the fourth to the seventh prestressings.

The specimen was prestressed next piecewise linearly to point D ($\sigma = 5909$ psi, $\tau = 0$, $\epsilon_x^{pl} = 4{\cdot}2$ μin/in, $\gamma_{xy}^{pl} = -12{\cdot}0$ μin/in) in the way indicated. Such a prestress path is of course not the exact Mises path but it is an approximation. The specimen was immediately unloaded to $\sigma = 5634$ psi, $\tau = 848$ psi within the new elastic region while no additional plastic and creep strains appeared. Then the fourth subsequent yield surface was obtained by means of two yield curves.

The specimen was now prestressed a fifth time piecewise linearly along an approximate Mises line to point E ($\sigma = 1795$ psi, $\tau = -3286$ psi, $\epsilon_x^{pl} = -9{\cdot}0$ μin/in, $\gamma_{xy}^{pl} = -145$ μin/in). The specimen was then immediately unloaded along the prestress path to $\sigma = 2968$ psi, $\tau = -2684$ psi and during this unloading, and while outside the yield surface an additional plastic strain $\epsilon_x^{pl} = 0$, $\gamma_{xy}^{pl} = -7{\cdot}7$ μin/in developed. The fifth subsequent yield surface was then obtained by means of two yield curves.

The fourth and fifth prestressing generated yield surfaces in the general area where they could be predicted to be located. However, no conclusions could be drawn concerning the question of

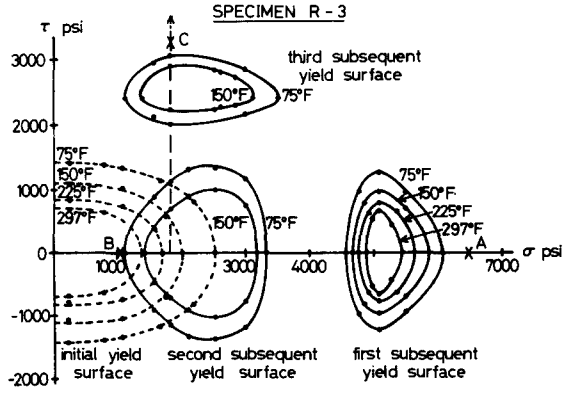

Fig. 4. Yield surfaces for specimen R-3. Part I. Initial and first three subsequent yield surfaces.

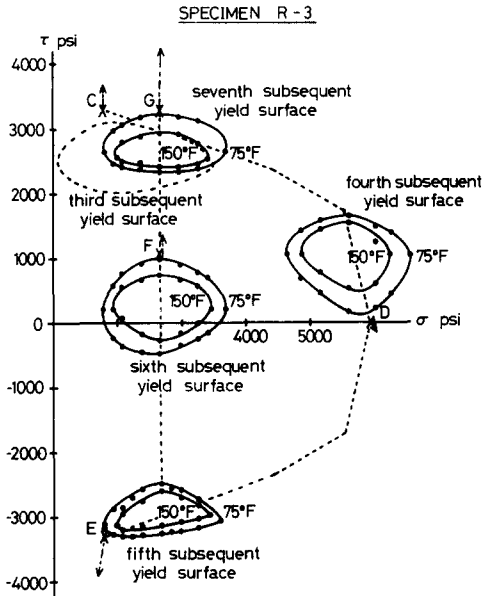

Fig. 5. Yield surfaces for specimen R-3. Part II. Fourth to seventh subsequent yield surfaces.

whether the Mises path is the global neutral loading path because between prestress points C and E only an insufficient number of yield surfaces were determined. In addition, for the same reason no conclusion could be drawn of whether the motion of the yield surface followed the hardening law enunciated earlier [3, 5].

The specimen was now prestressed for a sixth time to point F ($\sigma = 2675$ psi, $\tau = 1060$ psi, $\gamma_{xy}^{pl} = 29{\cdot}2$ μin/in). The specimen was immediately unloaded along the prestress path to $\sigma = 2675$ psi, $\tau = 530$ psi within the new elastic region. During this unloading and while outside the yield surface an additional $\gamma_{xy}^{pl} = 1{\cdot}6$ μin/in developed. The 6th subsequent yield surface was obtained by means of two yield curves.

The specimen was now prestressed a seventh time to point G ($\sigma = 2675$ psi, $\tau = 3286$ psi, $\epsilon_x^{pl} = 13$ μin/in, $\gamma_{xy}^{pl} = 372$ μin/in). The specimen was immediately unloaded along the prestress path to $\sigma = 2675$ psi, $\tau = 2862$ psi within the latest elastic range and an additional $\gamma_{xy}^{pl} = 6{\cdot}5$ μin/in appeared while unloading and while outside the yield surface. The seventh subsequent yield surface was then obtained by means of two yield curves. The sixth and seventh prestressing show vividly that the hardening law [3, 5] is valid.

After the nth yield surface was obtained in the process of prestressing to obtain the $(n+1)$th yield surface, the nth yield surface was intersected by the prestressing path and plastic strains started accumulating. Suppose, for example, that we are considering the fourth subsequent yield surface and the fifth prestressing to E. Figure 6 shows the development of the strains as prestressing progresses. Figure 6(a) gives the increase of the *total* normal strain as the axial stress changes. Figure 6(b) represents the development of the *total* shear strain as the shear stress changes. Finally Fig. 6(c) gives the development of the *plastic* strain as prestressing increases. It is seen that the plastic strain is only a shearing strain until the axial stress reaches the value of $\sigma = 4150$ psi.

Figure 6 can be used to produce a field of plastic strain rate vectors along the prestressing path. Indeed, in Fig. 5 we show the directions of the plastic strain rate vectors at selected points along the prestressing paths. These directions were determined from diagrams such as shown in Fig. 6. It is obvious that the plastic strain rate vectors must have different magnitudes. The magnitude of each plastic strain rate vector represents the rate of increase of the plastic strain as the stress increases. At the prestressing points D, E, F, G the plastic strain rate vector is always normal to the subsequently determined yield surface.

Specimen R-4. With one specimen we obtained, at room temperature, an initial yield curve, three subsequent yield curves, and we observed the development of the plastic strain rate vector and of the creep strain vector during six prestressings. Figures 7–9 show the results for the test.

The initial yield curve is shown in Fig. 7 and is similar to the ones obtained in the previous

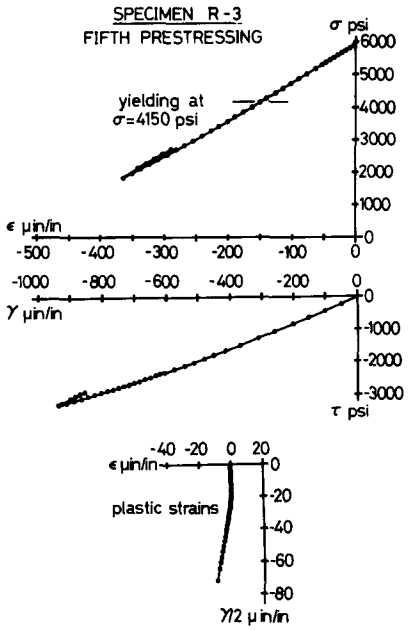

Fig. 6. Specimen R-3. Stress-strain diagrams for fifth prestressing.

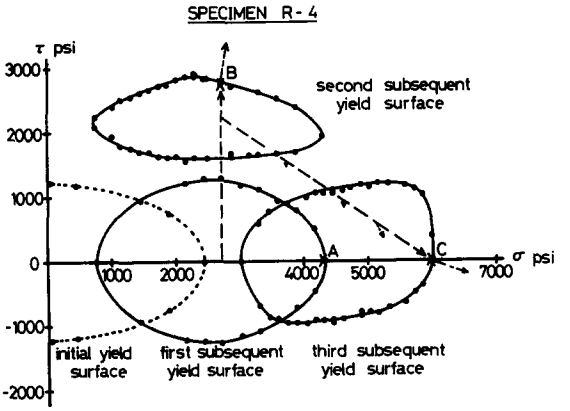

Fig. 7. Specimen R-4. Initial and subsequent yield surfaces.

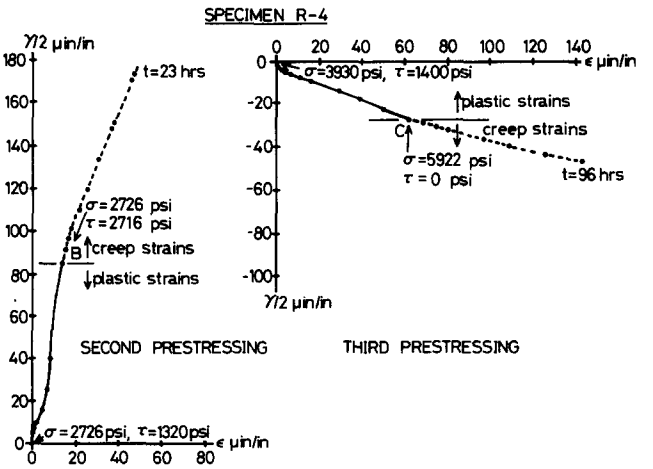

Fig. 8. Specimen R-4. Stress-strain diagrams for second and third prestressings.

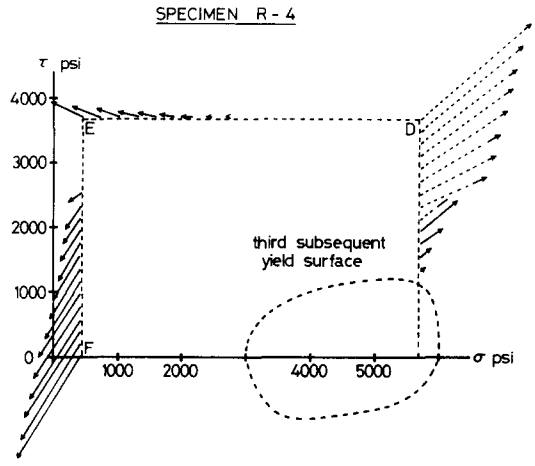

Fig. 9. Specimen R-4. Strain increment vectors for fourth to sixth prestressings.

test. The specimen was then prestressed to the point A at ($\sigma = 4288$ psi, $\tau = 0$, $\epsilon_x^{pl} = 3{\cdot}0$ μin/in) and it remained at the prestress point A for 2 hr while an additional axial creep strain $\epsilon_x^{cr} = 4{\cdot}7$ μin/in appeared. Then it was unloaded within the new elastic region and the first subsequent yield curve was obtained. The specimen was then subjected to a 2nd prestressing in torsion to the point B ($\sigma = 2767$ psi, $\tau = 2716$ psi, $\epsilon_x^{pl} = 13{\cdot}7$ μin/in, $\gamma_{xy}^{pl} = 171{\cdot}7$ μin/in). The specimen remained at the prestress point B for 23 hr and an additional creep strain of $\epsilon_x^{cr} = 37{\cdot}3$ μin/in, $\gamma_{xy}^{cr} = 173{\cdot}5$ μin/in appeared after which the 2nd subsequent yield curve was determined.

Next the specimen was prestressed for the third time to point C($\sigma = 5992$ psi, $\tau = 0$, $\epsilon_x^{pl} = 62{\cdot}6$ μin/in, $\gamma_{xy}^{pl} = -53{\cdot}6$ μin/in). It remained at C for 96 hr while the creep strain $\epsilon_x^{cr} = 80{\cdot}7$ μin/in, $\gamma_{xy}^{cr} = -38{\cdot}8$ μin/in appeared. The third subsequent yield surface was then determined.

We observe that in the test R-4 at the end of each prestressing the specimen was allowed to remain at the prestress point for considerable time while creep strain was developing. As expected from the model introduced in [5, 18] the yield surface would then pass very near the prestress point and this was indeed the case. In the first two prestresses the law of motion of the yield surface introduced in [3, 5] is valid. In the third prestress, however, there is a small deviation. A reason for this deviation may be that the prestress path to C intersects the second subsequent yield surface at a rather small angle. If the plastic rate vector has any influence on the development of the subsequent yield surface, its direction should influence the results.

In Fig. 7 the plastic strain rate vectors at selected positions in the stress path are shown. They have been obtained as indicated in the case of specimen R-3. Also the creep strains developed at the positions A, B and C are shown. We observe that normality is valid at B and C. In addition, if we assume that normality is valid throughout prestressing then the direction of the plastic strain rate vector determines the orientation of the yield surface element in its neighborhood as prestressing proceeds.

Figure 8 shows two curves representing the plastic and creep strains as they develop during the second and third prestressing. It is seen that the direction of the strain rate vectors and B and C are nearly identical to the directions of the creep vectors at these two points when creep starts developing. However, a small change in the direction of the creep vector gradually develops.

Three additional prestressings to D, E and F were performed, Fig. 9. The fourth prestressing D at $\sigma = 5708$ psi, $\tau = 3686$ psi produced plastic strains $\epsilon_x^{pl} = 5096{\cdot}8$ μin/in, $\gamma_{xy}^{pl} = 8993{\cdot}4$ μin/in.† The specimen remained at D for $47\frac{1}{2}$ hr developing creep strains $\epsilon_x^{cr} = 74{\cdot}7$ μin/in and $\gamma_{xy}^{cr} = 207{\cdot}3$ μin/in. The fifth prestressing to E at $\sigma = 454$ psi, $\tau = 3686$ psi produced plastic strains $\epsilon_x^{pl} = -3{\cdot}7$ μin/in, $\gamma_{xy}^{pl} = 3{\cdot}3$ μin/in. The specimen remained at E for 23 hr developing creep strains $\epsilon_x^{cr} = -12$ μin/in, $\gamma_{xy}^{cr} = 8{\cdot}8$ μin/in. Finally the sixth prestressing to F at $\sigma = 454$ psi, $\tau = 0$

†Note that in the computations of the plastic and creep strains we took into account the rotation of the strain gages due to large plastic deformations.

produced plastic strains $\epsilon_x^{pl} = -23{\cdot}3\ \mu$in/in, $\gamma_{xy}^{pl} = -74{\cdot}8\ \mu$in/in. The specimen remained at F for $40\frac{1}{2}$ hr developing creep strains $\epsilon_x^{cr} = -22\ \mu$in/in, $\gamma_{xy}^{cr} = -66\ \mu$in/in.

The directions of the plastic strain rate vectors along the path and the creep strain vectors at D, E and F are shown in Fig. 9. In addition, Fig. 10 shows the development of the plastic and creep strains during the fourth, fifth and sixth prestressings. Figures 9 and 10 show very vividly that substantial negative plastic strains are possible at stress points where σ and τ are both positive. While the specimen is subjected to a positive shearing stress and to a small axial tension it develops shearing strains of the opposite sign and is simultaneously shortened. This phenomenon is due to the fact that the yield surface moves in stress space following the prestress point and not enclosing the origin.

Figure 9 shows implicitly that our law of hardening is valid during the fourth prestressing. Indeed it is observed that during the fourth prestressing the yield surface must move upwards to pass by D. Now, when subsequently we have a fifth prestressing to E plastic strains start developing only after the stress path has reached a point which is such as if the four subsequent yield surface, which has not been determined, had a width in the direction DE equal to the width of the third subsequent yield surface in the same direction. This supports our hardening law. A similar observation can tentatively be made for the fifth prestressing.

Specimen R-6. With one specimen we obtained, at room temperature, an initial yield surface, and three subsequent yield surfaces. All four yield surfaces were obtained by means of one yield curve each. The initial yield curve is shown in Fig. 11 and is similar to the ones obtained in the

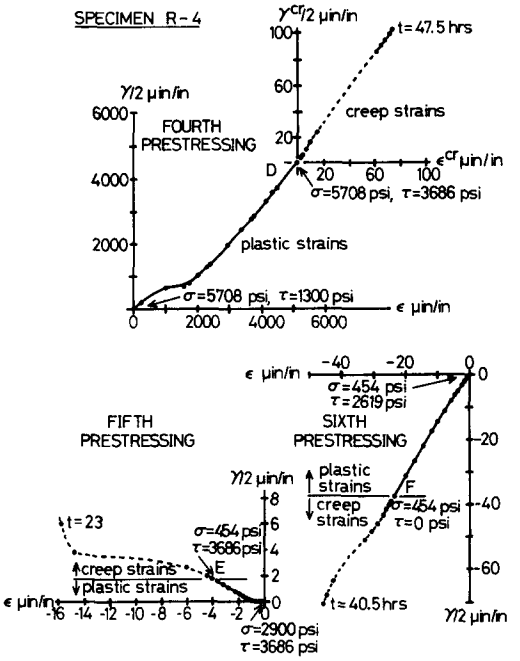

Fig. 10. Specimen R-4. Stress-strain diagrams for fourth, fifth and sixth prestressings.

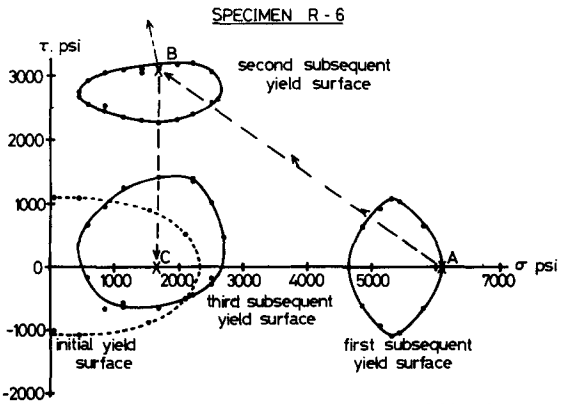

Fig. 11. Specimen R-6. Initial and subsequent yield surfaces.

previous tests. The specimen was then prestressed to the point A: ($\sigma = 6110$ psi, $\tau = 0$ with $\epsilon_x^{pl} = 20{\cdot}9$ μin/in). It remained at A for $23\frac{1}{2}$ hr and developed the creep strain $\epsilon_x^{cr} = 21{\cdot}0$ μin/in. Then the first subsequent yield surface was obtained.

After a second prestressing to the point B ($\sigma = 1686$ psi, $\tau = 3024$ psi, $\epsilon_x^{pl} = -6{\cdot}3$ μin/in, $\gamma_{xy}^{pl} = 48{\cdot}2$ μin/in) the specimen remained at B for $22\frac{1}{2}$ hr and developed creep strains $\gamma_{xy}^{cr} =$ 39 μin/in with a negligible axial creep strain. The second subsequent yield surface is also shown in Fig. 11. Finally after a third prestressing to the point C: ($\sigma = 1686$ psi, $\tau = 0$, $\gamma_{xy}^{pl} = -16{\cdot}2$ μin/in) the specimen remained at C for two weeks and then the yield surface was determined.

It is seen that the law of motion of the yield surface [3, 5] is valid in all prestressings in this specimen. Plastic strain rate vectors are shown at selected points in the paths. We observe that they are normal to the yield surfaces.

During the determination of the second and third subsequent yield surfaces we observed that the prestressing points B and C are inside the corresponding yield surfaces; B is slightly inside the 2nd yield surface but C is heavily so. This is, of course, the phenomenon of strain aging which is well known from simple tension tests but here we see it in combined stress tests.

As a final item in this section we add that an analytical study of the hardening law presented here has been given in a recent paper [21]. In this paper an analytical representation of the hardening law was presented. This analytical representation was applied to previous experimental data and an excellent agreement between analysis and experiment was shown. Finally the hardening law was compared with previously proposed hardening laws.

SOME ADDITIONAL RESULTS

In addition to the experiments concerning yield surfaces and normality, the investigation including some auxiliary experiments which will be discussed now. They were performed primarily with the square cross section specimens, but some were also performed with the tubular specimens.

The experimental program with the square cross section specimens was the following: Each of the seven specimens was stressed in pure tension until a particular range of total axial strain was reached. This range was approx. 8000 μin/in for specimens RA-1, 3-, -5, -6 which were tested at 70°F and 4000 μin/in for specimens RA-4, -7, -8 which were tested at ~200°F. Annealing of these specimens was at 650°F for specimens RA-1, -3, -4 and 1000° for specimens RA-5, -6, -7, -8.

Upon reaching the maximum stress, which was of course different for each specimen, the specimens were all held at that value of stress for 1000–1200 min while creep strains occurred. Then the specimens were unloaded to $\sigma = 240$ psi at the same incremental rate as used in loading and were allowed to remain at that stress level for 200 min while unloading creep occurred.

We observed that the yield limit decreases with increasing annealing temperature. Since with increasing annealing temperature, the rates of grain growth and of reduction of dislocation density are increased the experimental results are plausible. We can assume that at a higher annealing temperatures the specimens have larger grains and lower dislocation density.

We also observed that the yield point decreased with increasing test temperature. If a linear relation between yield point value and testing temperature would be assumed to be valid as the testing temperature decreases, then the yield point would become zero at $T_{cr} = 600$°F for both annealing temperatures. Even for the tests with the tubular specimens which were annealed at 650°F we can draw the conclusion that $T_{cr} = 600$°F.

The next question to be discussed is the verification of the constant volume hypothesis for plastic and creep strains when the range of plastic and creep strain is less than 1%. A literature search revealed that only a few studies on this matter were available and this verification was necessary for the computation of the plastic strains for the tubular specimen.

The physical argument for the assumption of incompressibility is that the basic mechanism of plastic strain is simple slip and when slip occurs in a crystal the volume remains the same. This model neglects, however, the effect of the grain boundaries in the polycrystal and the dislocation generation within the grains.

The value of the sum $\epsilon_x^p + \epsilon_y^p + \epsilon_z^p$ at the end of each loading period varies from 240 μin/in for the specimens tested at 70°F which exhibited a total axial strain of the order of 8000 μin/in, and from -180 μin/in to 43 μin/in for the specimens tested at 200°F which exhibited a total axial strain of the order of 4000 μin/in. It is seen that the values of this sum are very small compared to

the values of the axial plastic strains. Thus, the constant value hypothesis is essentially valid for both testing temperatures and both annealing temperatures. In this context it is interesting to note that the specimens with the higher annealing temperature or higher testing temperature gave the greater departure from the constant volume hypothesis. A tentative explanation of this result is as follows: All specimens were made from extruded aluminum with a high dislocation density and small grain size due to the plastic strains generated by the extrusion process. Since annealing reduces the dislocation density and causes an increase in grain size it follows that specimens annealed at 650°F would have a higher dislocation density and smaller grain size than those annealed at 1000°F. Now as the specimens are plastically strained, the dislocation density rises and eventually reaches a saturation level of 10^{12} lines per cm^2; however, these *generated* dislocations result in lattice distortions which cause strains that do not necessarily preserve volume. Specimens annealed at the higher temperature would have a larger change in dislocation density due to testing and hence a greater departure from the constant volume hypothesis. Similarly, testing at higher temperatures produces a larger change in dislocation density and a similar result as above will appear.

We also remark that for both testing temperatures as the annealing temperature is raised, the magnitude of the plastic strains for a given stress increases. Similarly, for both annealing temperatures as the testing temperature is raised the magnitude of the plastic strains increases.

Although for plastic strains the constant volume hypothesis seems to be esentially substantiated by these experiments, for the creep strains we have a different conclusion. From Figs. 12 and 13, which are typical, at the beginning of the loading creep test the creep strains do preserve volume; however, as the loading creep test continues there is a serious departure from the constant volume hypothesis. This changing behavior with time is similar with the time-dependent changing direction of the creep strain vector observed for the tubular specimens. Figures 12 and 13 illustrate two typical loading creep tests. It should be added that the departure

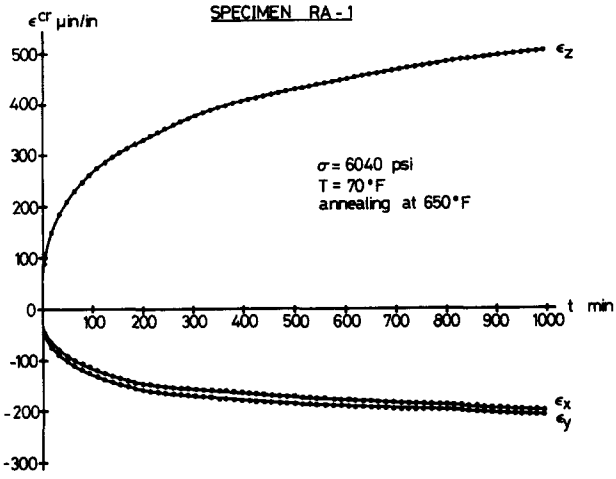

Fig. 12. Development of creep strains for specimen RA-1. Test temperature $T = 70°F$, Annealing at 650°F.

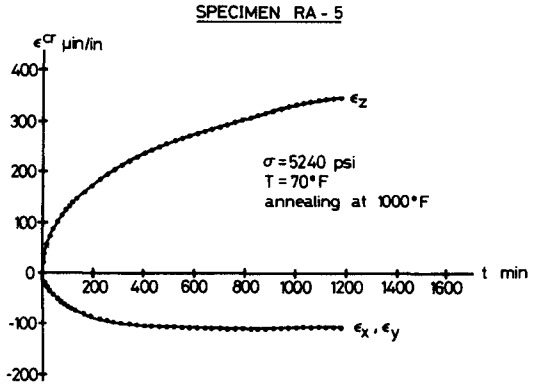

Fig. 13. Development of creep strains for specimen RA-5. Test temperature $T = 70°F$. Annealing at 1000°F.

from the constant volume hypothesis for creep strains can only last for a limited period of time which, however, exceeds the duration of our experiments.

The next question to be considered is the relation between plastic strain and creep strain. Is there any fundamental difference between plastic strain and creep strain? From the experiments with tubular specimens we observed that the creep strain rate vector has the same magnitude and direction as the plastic strain rate vector at the stage where the incremental loading stops and creep starts. Hence, creep is initially a continuation of plastic flow. Later, however, the direction and magnitude of the creep strain rate vector changes gradually from that which exist at the initiation of creep. Therefore, during creep additional mechanisms of deformation may be successively entering the picture.

Additional experimental evidence is given in Fig. 14 in which a typical stress-change in strain diagram is plotted. Here, the strain axis illustrates the change in strain which occurred during the time the specimen remained at a particular stress. It is seen that below yield, as defined by us[1–3], no change in the strain readout occurred with time whereas for stresses above yield, both a plastic and creep strain are present. Hence creep and plastic strains start simultaneously. This phenomenon appeared in all tests, for both the tubular and square cross section specimens.

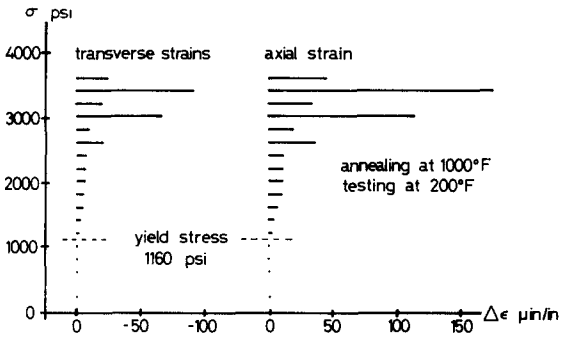

Fig. 14. Simultaneous initiation of plastic and creep strains.

CONCLUSIONS

In this paper we added significantly to our previous knowledge on the experimental foundations of plasticity. With the help of a number of combined stress experiments on commerically pure aluminum 1100-0 we have shown that our previously stated law of hardening[3, 5, 6] is valid for three complicated prestressing paths in the tension-torsion space, except possibly when the prestress path intersects the yield surface at an angle which is very small. This last question is the subject of a current investigation.

Next we have shown that the normality assumption between the yield surface and the plastic strain rate vector is valid. We also investigated the development of creep after prestressing. We have shown that the creep strain vector has in the beginning the same direction as the plastic strain rate vector but that later its direction may change. Finally, we have shown that at the level of permanent strains less than 1% the plastic strains follow the constant volume hypothesis but the creep strains do so only when they begin to appear.

REFERENCES

1. A. Phillips, Yield surfaces of pure aluminum at elevated temperatures. *Proc. IUTAM Symp. on Thermoinelasticity* (Edited by B. A. Boley), pp. 241–258. Springer, Berlin (1970).
2. A. Phillips, C. Liu and J. Justusson, An experimental investigation of yield surfaces at elevated temperatures. *Acta Mech.* **14**, 119 (1972).
3. A. Phillips and J. Tang, The effect of loading path on the yield surface at elevated temperatures. *Int. J. Solids Struct.* **8**, 436 (1972).
4. A. Phillips and R. Kasper, On the foundations of thermoplasticity—An experimental investigation. *J. Appl. Mech.* **40**, 891 (1973).
5. A. Phillips, Experimental plasticity. Some thoughts on its present status and possible future trends. *Problems of Plasticity* (Edited by A. Sawczuk), pp. 193–233. Int. Symp. on Foundations of Plasticity (1972).
6. A. Phillips, New theoretical and experimental results in plasticity and creep. *Proc. 2nd Int. Conf. on Structural Mech. in Reactor Technology*, Vol. V, Part L/3/6 (1973).
7. P. Naghdi, F. Essenburg and W. Koff, An experimental study of initial and subsequent yield surfaces in plasticity. *J. Appl. Mech.* **25**, 201 (1958).
8. W. Prager, A new method of analyzing stress and strain in work-hardening plastic solids. *J. Appl. Mech.* **23**, 493 (1956).

9. I. U. Ishlinskii, General theory of plasticity with linear strain-hardening. *Ukr. Ing. Zh.* **6**, 314 (1954).
10. P. G. Hodge, Jr., Discussion of Ref. 8. *J. Appl. Mech.* **24**, 482 (1957).
11. H. Ziegler, A modification of Prager's hardening rule. *Q. Appl. Math.* **17**, 55 (1959).
12. A. Baltov and A. Sawczuk, A rule of anisotropic hardening. *Acta Mech.* **1**, 81 (1965).
13. H. Ivey, Plastic stress-strain relations and yield surfaces for aluminum alloys. *J. Mech. Engng Sci.* **3**, 15 (1961).
14. S. Batdorf and B. Budiansky, A mathematical theory of plasticity based on the concept of slip NACA TN 1871, 1–33 (1949).
15. G. I. Taylor and H. Quinney, The plastic distortion of metals. *Phil. Trans. Royal Soc. London*, Ser. A (230), pp. 323–362 (1931).
16. J. Miastkowski and W. Szczepinski, An experimental study of yield surfaces of prestrained brass. *Int. J. Solids Struct.* **1**, 189 (1965).
17. W. M. Mair and H. Ll. D. Pugh, Effect of prestrain on yield surfaces in copper. *J. Mech. Engng Sci.* **6**, 150 (1964).
18. A. Phillips, J. L. Tang, M. Ricciuti, Some new observations on yield surfaces. *Acta Mech.* **20**, 23 (1974).
19. R. L. Sierakowski and A. Phillips, The effect of repeated loading on the yield surface. *Acta Mech.* **6**, 217 (1968).
20. G. M. Brown, Inelastic deformation of an aluminum alloy under combined stress at elevated temperatures. *J. Mech. Phys. Solids* **18**, 383 (1970).
21. A. Phillips and G. J. Weng, Study of an experimentally verified hardening law. *J. Appl. Mech.* **42**, 375 (1975).